Coupled CFD-Simulation of a Helicopter in Free-Flight Trim

Martin Embacher*, Manuel Keßler*, Markus Dietz**, Ewald Krämer*
Ph.D. Student   Research Associate   R&D Engineer   Professor

* IAG, Universität Stuttgart, Pfaffenwaldring 21, 70550 Stuttgart, Germany
** Eurocopter Deutschland GmbH, München, Germany

e-mail: embacher@iag.uni-stuttgart.de, kessler@iag.uni-stuttgart.de

ABSTRACT

This paper presents a feasibility study for trimming the computational fluid dynamics model of a complete helicopter to free flight conditions by coupling it to a comprehensive rotor code. Rotor controls and fuselage pitch and yaw attitude are set as free trim variables to realize load equilibrium for a steady cruise flight condition. Through weak fluid-structure coupling aeroelastic effects at the main rotor are accounted for, while fuselage loads are transferred in form of temporal mean values. Aerodynamic simulation of the Eurocopter EC145 helicopter fuselage is characterized by separated and partially irregular flow, and interference between rotor and fuselage renders flight mechanics rich in non-linearity. Special attention therefore is given to the convergence rate, precision and stability of the expanded trim scheme. The work is motivated by an expected gain in the prediction capability for helicopter performance and interactional loads from exploiting high-fidelity aerodynamic modeling simultaneously for flight attitude prediction.

NOTATION

CFD	Computational Fluid Dynamics
DLR	Deutsches Zentrum für Luft und Raumfahrt
FLOWer	DLR's structured Finite-Volume flow solver
IAG	Institut für Aero- und Gasdynamik, Stuttgart
HOST	Helicopter Overall Simulation Tool

θ_0	Main rotor collective blade pitch
$\theta_{C,S}$	Main rotor cyclic blade pitch
$\theta_{0,TR}$	Tail rotor collective blade pitch
C_T/σ	Tail rotor thrust coefficient over solidity
Ψ	Helicopter yaw attitude, positive nose right
Θ	Helicopter pitch attitude, positive nose up
Φ	Helicopter roll attitude, positive right

F_{3D}^n	CFD loads transferred to HOST at trim n
F_{2D}^n	HOST-internal aerodynamic loads at trim n
F_{HOST}^n	Loads employed by HOST at trim n

$C_{x,y,z}$	Force coefficients,
$C_{Mx,My,Mz}$	Moment coefficients about hub center,

in the helicopter system of reference:

x	Pointing upward
y	Pointing rearwards
z	Pointing to the right

INTRODUCTION

The numerical simulation of rotor flow for helicopter applications generally is a threefold problem, since it not only consists in solving for the flow field itself, but also in accounting for the aeroelasticity of the rotor blades and simultaneously in reaching a trimmed state of the rotor. Aeroelasticity is realized by coupling the flow solver with structural computation, and is closely linked to the rotor trim state. Depending on the number of control inputs set free, trim assures that an equal amount of rotor parameters meet realistic trim objectives. In its standard application, trimming an isolated rotor means adjusting the collective and cyclic pitch angles in order to fulfill a trim law comprised of three objectives. Typically, average thrust and the rolling and pitching moment generated by the rotor are required to meet certain fixed target values. A review on fluid-structure coupling efforts on isolated rotors is found in [1].

CFD simulations of isolated rotors using fluid-structure coupling and trim along three degrees of freedom have been routinely employed at our department for some years and were geared towards the reproduction of wind tunnel experiments or the comparative study of active rotor concepts [2]. For these applications, the three component trim in conjunction with an adequate number of aeroelastic degrees of freedom was considered sufficient to ensure the similitude of the dynamic and aerodynamic state of the rotor.

Applying this simulation environment to rotors in free flight condition, however, calls for an expansion of the trim procedure. In contrast to rotor stand tests in wind tunnels, the helicopter attitude varies to establish the load equilibrium for the entire helicopter in free flight.

Accordingly, it is appropriate to expand the procedure by trimming two further degrees of freedom at the main rotor, namely the lateral and longitudinal mast orientation angles, accompanied by two additional trim objectives standing in close relation to the mast angle.

Unlike the "wind tunnel trim" the free flight trim features non-constant and a-priori unknown objectives for the rotor. Requiring equilibrium of all loads acting on the complete helicopter for a chosen stationary flight condition, entails, from the main rotor's perspective, the necessity to balance the fuselage drag and moments. These vary with helicopter attitude, and any change in attitude alters both rotor and fuselage loads in a non-linear manner. To find the equilibrium position, the same iterative solution procedure as for trimming the remaining degrees of freedom is used in the present case to fulfill the load equilibrium in the mean, i.e. the fuselage sustains no vibratory rigid or elastic body motion. Principally, two sources of fuselage aerodynamic loads can be used for free flight trim. Loads are either solely estimated from tabulated data directly accessed by the trim scheme, or they alternatively are obtained from CFD and coupled into the scheme as corrective term in the sense of the delta trimming procedure. In the first case, usually only the isolated rotor is modeled by CFD, whereas in the second approach CFD solves the flow field around a complete helicopter configuration, and the entire spectrum of interactional phenomena [3] represented in CFD is accounted for in the trim procedure. While the first approach was tested for convergence in a preparatory step [4, 5], the present study considers the full problem with aerodynamic loads for both rotor and fuselage obtained from CFD. In trimmed state, the entirety of aerodynamic loads is in balance with helicopter weight in the temporal mean, with dynamic equilibrium established at the rotor blades.

Previous work in the direction of free flight trim was presented in [6] and [7], where trimming the mast orientation was included in the coupled isolated rotor simulation to predict vibratory loads for level flight cases of the UH-60A Airloads Program. Fuselage loads were obtained from wind tunnel experiments in this reference. Also in the context of the UH-60A program, and investigating a steady as well as an unsteady maneuvering flight condition, a tight fluid-structure coupling scheme at the rotor blades was embedded in an inverse flight mechanics simulation in [8]. Again, the isolated rotor was simulated and fuselage aerodynamic loads were obtained from table look-up. Reference [9] includes the fuselage in the CFD model of a tandem helicopter configuration, but in trimming an empirical model for fuselage lift, drag and pitching moment was used. Thus, the displacement effect of the fuselage on the rotors influenced the trim, while the action of interference on the fuselage was not accounted for in trimming. An interesting approach to free flight trim, were tabulated fuselage data is used in conjunction with CFD determined interference loads, was recently presented in [10]. Steady flow simulations with and without actuator disk provided the load component due to interference. For various flight conditions of an NH-90 like configuration the impact of rotor-fuselage interaction on the trim state was estimated. Reference [5] presented free flight trim results for the EC145 helicopter in a flight condition comparable to the present study. An isolated rotor was modeled in CFD and weakly coupled to a comprehensive rotor code which provided the empirical fuselage aerodynamic model.

The paper is organized as follows. An outline of the expanded weak coupling and trim scheme is followed by a study of skid-fuselage interference effects, aiming at the omission of the skids. In the main part the applied procedure of free flight trimming is stated, and convergence rate, accuracy, computational effort, and stability issues of the scheme are examined. Remarks with respect to the flight test reference conclude the paper.

NUMERICAL MODELS

Flow Solver

The CFD solver FLOWer was compiled by DLR in the framework of the MEGAFLOW project [11] and is available at IAG through the cooperation with DLR e.g. in the CHANCE [12] and SHANEL [4] projects.

FLOWer solves the three-dimensional, compressible and unsteady Reynolds-Averaged Navier-Stokes equations using a Finite Volume method on block-structured meshes. The equations are formulated in a non-inertial rotating reference system with explicit contributions of centrifugal and Coriolis forces to the momentum and energy equations. FLOWer includes a cell-vertex and a cell-centered formulation. Convective fluxes are computed using the JST scheme [13] which uses 2nd order central differences with artificial dissipation for stabilization. In order to circumvent the time step limitation of the explicit time integration scheme, FLOWer makes use of the dual time stepping technique with a second order implicit time integration operator in case of unsteady flow [14]. The integration in pseudo time is carried out using a 5-stage hybrid Runge-Kutta method. Furthermore, FLOWer includes the Arbitrary Lagrangian-Eulerian (ALE) formulation which facilitates the computation of deforming meshes by adding whirl-fluxes resulting from the cell face motion to the convective flux portion. The Geometric Conservation Law (GCL) evaluates the cell volumes of the deformable mesh consistent to the cell face velocities. This ensures the preservation of uniform flow on deformable grids. The Chimera-technique allows for arbitrary relative motion of aerodynamic bodies [15]. Chimera connectivity is determined using hole cutting and interpolation. The Alternating Digital Tree (ADT) search method is applied in order to identify donor cells in curvilinear grids.

Within the past years additional helicopter specific features have been integrated into FLOWer mainly by IAG [16]. This includes interfaces for time-accurate and weak

coupling on helicopter main rotors, a deformation tool for multi-block blade grids and rotor specific post-processing. The work presented in the present paper represents the continuation of IAG's efforts to continuously improve the helicopter computational environment using the FLOWer solver.

Aeromechanics Code

Eurocopter's in-house comprehensive rotorcraft code HOST [17] is mainly used for flight mechanics purposes and enables the study of single helicopter components like isolated rotors as well as complete configurations with related substructures. HOST trims the rotor based on a blade element formulation with 2D airfoil tables. Airframe component aerodynamics is provided by polars. For stand alone simulations interference models are available in order to account for the interference effects between the individual components of the helicopter in certain flight conditions. HOST includes an elastic blade model which considers the blade as a quasi one-dimensional Euler-Bernoulli beam. It allows for deflections in flap and lag direction and elastic torsion along the blade axis. In addition to the assumption of a linear material law, tension elongation and shear deformation are neglected. However, possible offsets between the local cross-sectional centre of gravity, tension centre and shear centre are accounted for, thus coupling bending and torsional degrees of freedom. Rigid segments are connected through virtual joints, allowing for geometrical nonlinearities. The large number of local relocations as degrees of freedom is reduced by a modal Rayleigh-Ritz approach, incorporating only a limited number of lower frequency modes and corresponding eigenforms. Accordingly, blade deformation is expressed as

$$h(r,\psi) = \sum_{i=1}^{n} q_i(\psi) \cdot \hat{h}_i(r),$$ **eq. 1**

where n is the number of modes, q_i the generalized coordinate of mode i (a function of the azimuth angle ψ), and $\hat{h}_i$ is the mode shape (a function of the radial position r). It is obtained by an eigenvalue analysis of the beam in vacuum, resulting in coupled flap/lag mode shapes and decoupled torsion modes.

Fluid Structure Coupling and Trim

Load transfer from CFD to the comprehensive helicopter code HOST is realized within a weak coupling framework, i.e. periodic loads are exchanged. Conversely, the set of trim variables calculated by HOST and forwarded to the flow solver equally describes a periodic state. The idea of the iterative weak coupling procedure is as follows: HOST uses the loads from CFD to correct its internal lower order aerodynamic model and then calculates an update of the trim state. In the present case of free flight trim, loads provided by FLOWer also comprise the fuselage loads, while the set of trim variables consists not only of the blade motion data and rotor control angles, but also of the fuselage

attitude angles. A schematic of the data exchange is given in Figure 1. In the current implementation, the radial and azimuthal distributions of blade sectional lift, drag and pitching moment calculated by FLOWer are delivered to the HOST blade modeling routines in form of line loads. They are Fourier filtered in time excluding harmonics of the main rotor frequency above the 10th. Blade motion resulting from aerodynamic correction and re-trim of the rotor is forwarded to FLOWer as a set of generalized coefficients q_i. The underlying basis of modal shapes consists of three flap modes, three lead/lag modes and two torsion modes. Motion is resolved up to the fifth harmonic in time. Fuselage loads from a complete helicopter simulation in FLOWer are time averaged and sorted per helicopter component, such as cabin, horizontal and vertical control surfaces, to be attributed to the respective HOST internal model. Although the sorting of loads is not necessary since finally, in trimmed state, the CFD loads completely replace the HOST aerodynamic model, it proves useful in tracing modeling discrepancies between FLOWer and HOST. As indicated in Figure 1, the coupling environment also allows to include loads from different, non-CFD, sources into the set of steady loads transferred to HOST. Presently, this feature is used to introduce estimates for skid and hub loads which are not modeled in CFD. No load coupling at the tail rotor is implemented to date.
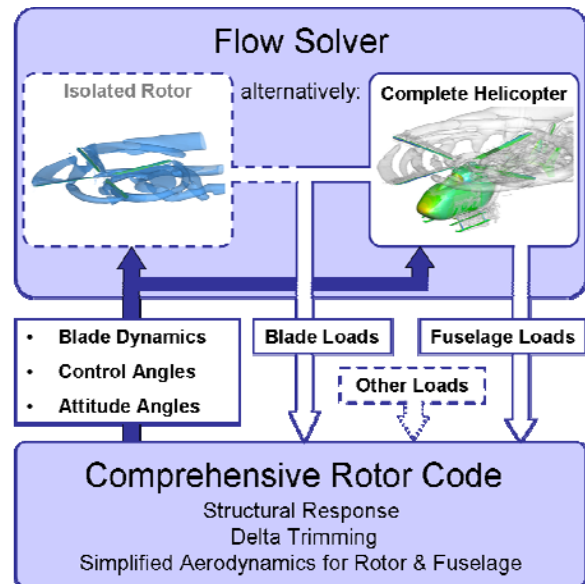

Figure 1: Schematic of data exchange between flow solver and aeromechanics code.

The specific steps of the coupling procedure are as follows:

1. HOST determines an initial trim state based on its internal aerodynamics. This state is termed "trim 0".

2. FLOWer calculates loads for the blade motion and fuselage attitude provided by HOST. Therefore, this stage also pertains to the current trim cycle "trim 0".

3. In the subsequent trim iteration, HOST employs the FLOWer load data to correct its internal aerodynamics. Accordingly, load coupling is implemented by setting

$$F_{HOST}^{n+1} = F_{2D}^{n+1} + \left(F_{3D}^n - F_{2D}^n \right). \qquad \textbf{eq. 2}$$

Superscript n denotes the trim iteration count, and F_{3D}^n and F_{2D}^n are the CFD and HOST loads from the previous cycle, respectively. Their difference represents the aerodynamic correction applied. In the current trim iteration n+1, trim variables are adjusted such that internal aerodynamic loads F_{2D}^{n+1}, corrected by the term in brackets, yield a load F_{HOST}^{n+1} that fulfills the trim objective.

4. FLOWer loads for the trim n+1 are calculated.

Steps 3 and 4 are repeated until convergence of the trim variables. At this point, no change in F_{2D} takes place from trim n to trim n+1, and CFD loads entirely replace the HOST aerodynamic model, $F_{HOST}^{n+1} = F_{3D}^n$.

Simulation Setup

The CFD mesh system is composed of 11 Chimera multi-block grid structures, the fuselage mesh, four main rotor blade meshes, two tail rotor blade meshes and four additional grid structures used for the skid landing gear. Table 1 lists the dimensions of each component. The fuselage mesh serves as a background mesh, i.e. it expands to the far field where characteristic boundary conditions are prescribed.

Table 1: Dimensions of grid system

	Blocks	Cells
Main rotor blades	4 x 30	4 x 1.750.016
Fuselage	65	8.487.680
Skids	104	6.936.064
Tail rotor blades	2 x 8	2 x 1.335.552
Total	305	25.094.912

The landing gear is not included in the fuselage mesh, but it is attached to the cabin bottom side using Chimera with overlapping walls. This strategy was chosen as it allows for an improved mesh quality and easy removal of the skid landing gear from the overall Chimera system. Auxiliary hole grids surrounding the cross tubes and the skids are defined in order to blank cells of the fuselage mesh located inside the landing gear geometry. At the overlapping wall area around the cabin-skid junction, surface patches with coinciding boundaries are defined in the fuselage mesh and the attached cross-tube meshes to enable a correct load evaluation.

In contrast to isolated rotor coupling and trim, a special challenge arises when extending the procedure towards complete helicopter trim. The helicopter attitude is subject to changes during the coupling and trim process, resulting in varying inflow angles relative to the helicopter. This has to be accounted for in the CFD simulation. Principally different methods can be applied for this purpose: When using a dedicated background mesh and Chimera near-field meshes for all helicopter components, Chimera components can directly be rotated within to the background mesh while conserving the inflow direction relative to the background. During restart of the solver from a preceding run with a different helicopter attitude, the flow direction update enters the near field meshes at their boundary by interpolation from the background mesh, and the solution develops from the previous flow state as initial condition. For the present mesh system this procedure is not possible as no dedicated background mesh is used. Another disadvantage of this method is the altered overlapping situation between child meshes and background mesh, possibly resulting in an increasing number of Chimera orphan points.

The second approach is to adjust the inflow direction on the helicopter by an adaption of the far field flow direction at the outer mesh boundaries. The major disadvantage of this method is the significant amount of time required to convect the altered inflow direction through the entire mesh system (propagation speed limited to $v_\infty + c$), which lasts about 1.5 rotor revolutions for the chosen extent of the computational domain. One way to circumvent this issue is to use whirl fluxes for the reorientation of the flow. This approach is used for the computations presented in this paper. Effectively, the helicopter is unsteadily piloted from its previous attitude into its new attitude using a specified number of physical time steps for this transition process. In the present study, the duration of the transition phase is set to one quarter of a main rotor revolution, thus maintaining acceptable angular velocities of the helicopter not exceeding 104°/sec. This strategy has proven to work well and features docile restart characteristics of the flow solver.

A physical time step of 1° main rotor azimuth has been chosen for all simulations, based on the satisfactory results with this resolution in previous applications of weak coupling to isolated main rotors. Note that this time step however corresponds to a low equivalent temporal resolution on the tail rotor as it rotates at a non-integer rpm ratio of 5.66 compared to the main rotor. Approximately 30 inner iterations were used to converge in pseudo time. For the closure of equations the Wilcox kω turbulence model was selected. See [18] for a comparison of different turbulence models and wind tunnel data for the EC145 fuselage. The simulated flight case is a steady forward flight condition at 136kts, and an impression of the vortex system can be gained from the λ_2 visualization in Figure 2.
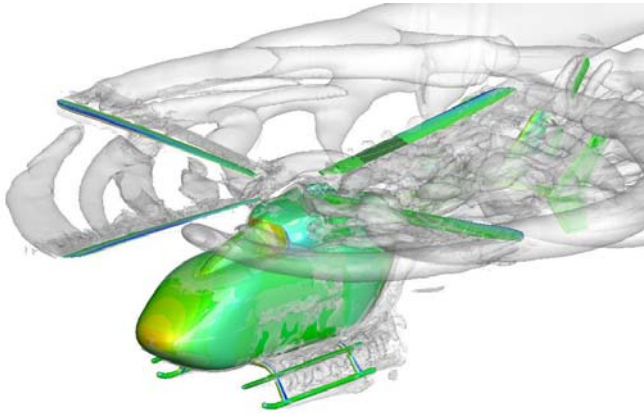
Figure 2: FLOWer simulation of EC145 helicopter

SKID-FUSELAGE INTERFERENCE

Including skids by means of overlapping grids not only increases flow solving effort by enriched detail, but also entails high computational effort at the boundary of the component grids to facilitate the flow data exchange. In the current implementation of the Chimera searching technique in FLOWer the calculation of connectivity relations for components remaining stationary within the background grid is repeated at every physical time step, despite the relations remaining identical. Hence, not only for the blades, but also for the skids, a considerable fraction of simulation time is spent for the search of donor cells in the non-Cartesian background mesh and the interpolation of the data onto the fringe layers of the component grid. This is particularly the case on vector computers, since the Chimera functionalities are not completely vectorized. For the present case and including the skids, Chimera effort compares to flux computation in a wallclock time ratio of 1.1 when computing on 16 processors of the NEC-SX9 vector computer. Hence, only about 47% of wallclock time is spent on flux calculation. With only the main and tail rotor blades remaining as embedded components, the ratio further rises to 1.4. Nevertheless, with a reduction in chimera and flux calculation efforts by 44% and by 56%, respectively, the omission of the skids speeds up the simulation by a factor of approximately 2 in case of the NEC-SX9. Consequently, and in light of the expected high demand of simulated time necessary to converge the free flight trim, it was decided to omit the skids. With only few experience gained previously with the expanded trim scheme, this step is also justified by the intention to focus on convergence matters. Nevertheless, the skids bear high relevance for a correct modeling of the helicopter's flight mechanics, notably the pitching moment balance, and therefore it was resorted to the compromise of retaining the skid influence through a fixed load correction. This correction enters the load transfer to HOST as described in the previous paragraph, and it is based on a study of skid loads and fuselage interference effects for the trim 0 flight condition. For a nose-left yaw attitude of $\Psi = -1.62°$, a nose-down pitch of $\Theta = -0.63°$ and a left roll of $\Phi =$

-2.26°, one simulation dispensing of the skids and one including them was carried out. Setup is identical apart from splitting one block of the mesh system and besides differences in the initial condition. The computation including the skids was restarted from a mesh testing run; it therefore incorporates a slight reorientation of the fuselage towards the trim 0 attitude at its beginning, i.e. the above described unsteady turning of the fuselage was applied. The simulation without skids is restarted at correct attitude from a fairly converged solution, but the initial condition pertains to a mesh system without trim tabs at the main rotor blades. Disturbances from the unsteady turn and the changed blade mesh were allowed to settle during two and one revolution, respectively. Subsequently, mean loads were determined by averaging over three revolutions, an interval which is hoped to be sufficient to even out any possible relics of the initial disturbances. Skid loads and, by forming the difference of averaged loads, the local influence from the presence of the skids on various parts of the fuselage is determined. Results are summarized in Figure 3, showing the effect on force coefficients, and in Figure 4, showing the impact on the moments for selected fuselage components. All loads are given relative to the helicopter system of reference which has the rotor mast rotated forward out of the x-axis by 5°, with the moment coefficients referring to the hub center.
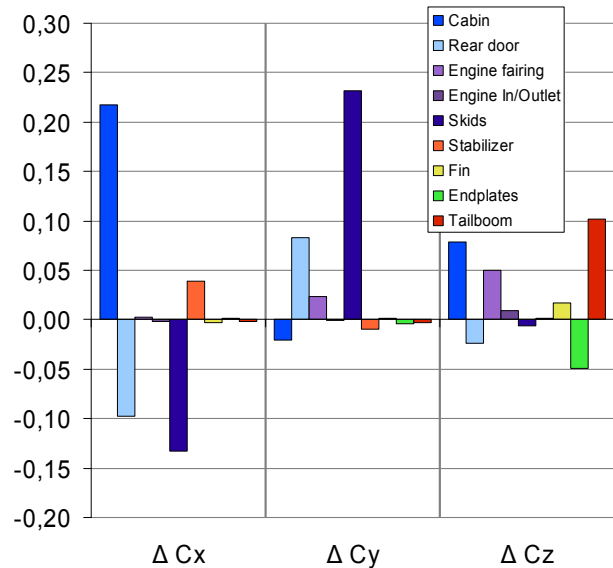

Figure 3: Skid loads and interference effect on fuselage due to inclusion of skids, force coefficients.

As expected, the main part of drag increase ΔCy originates at the skids themselves, and most of the interference induced drag increase is contributed by the rear door. Skid drag is directly linked to a negative pitching moment ΔC_{Mz} about the hub center. Partly due to nose-down pitch attitude and to flow deflection by fuselage and rotor downwash, a downward force $\Delta C_x < 0$ is generated on the skids. Vertical load balance however is nearly restored by interference effects, where particularly the additional positive lifting loads exerted on the cabin over-compensate the downward force generated on the rear door. A

considerable part of the skids' lifting effect on the cabin stems from the skid-fuselage interconnect, where the pressure rise extending upstream of the skid bars outweighs pressure losses in their wake due to separation. Not accounting for interferential stabilizer lift, virtually no change in vertical load is inferred through the skids.
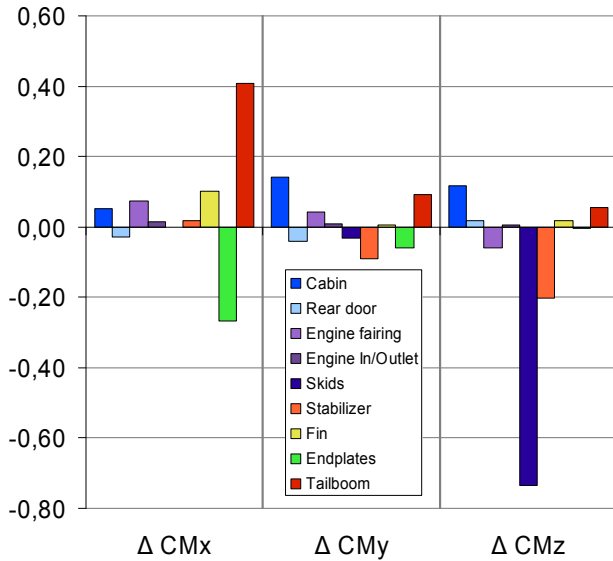

Figure 4: Skid loads and interference effect on fuselage due to inclusion of skids, moment coefficients.

Despite the moderate nose-left yaw attitude of $\psi = 1.62°$, considerable sideward forces and yawing moments are generated. Unlike drag and lift, the lateral force arising directly at the skids is inferior compared to the additional loads ΔC_z generated on nearly all components by the interference. Asymmetric base flow might show strong asymmetric reaction in response to the disturbances introduced by the skids, such as lateral replacement of separation lines.

Indication for a modified separation pattern can be found in Figure 5, were the modification in surface pressure due to the skids is plotted. The elongated areas of strong pressure changes at the tail boom probably are caused by a circumferential relocation of the wake vortices, which are formed at the rear door and engine fairing and are shed close to the tail boom protrusion. A strong sideward force to the right and the related yawing moment is generated at the tail boom. Further parts of the empennage are affected by changes in the wake and show reactions in rolling moment ΔC_{My}. However, since one of the simulations starts with an unsteady reorientation of the fuselage a connection of the asymmetry to this disturbance also can not be ruled out definitely. Furthermore, with respect to changing fuselage attitudes while trimming, the question arises whether the asymmetric effect of interference is sufficiently consistent with trim change. Due to the uncertainty about the origin and persistence of the significant lateral forces and yawing moments caused by the presence of the skids, no asymmetric

interference loads were included in the coupling. Only ΔC_x, ΔC_y and ΔC_{Mz} gain corrective influence on the fuselage aerodynamic calculations within HOST. If lateral skid load components and the full interference effect were retained, an asymmetry induced change in yaw attitude of additional 0.5° nose-left would result for trim 1.
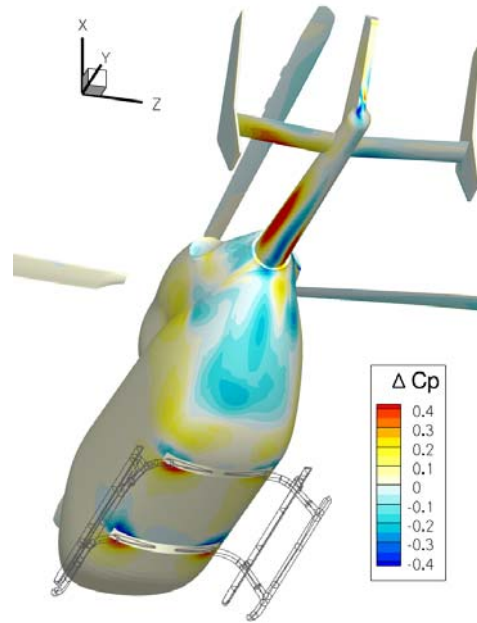

Figure 5: Difference in surface pressure due to the presence of skids.

TRIM CONVERGENCE

General Procedure

Based on the available flight test data from Eurocopter, which includes measurements of the fuselage pitch and roll attitude but lacks a recording of the yaw angle, a trim law that prescribes the roll angle to $\Phi = -2.26°$, i.e. roll left, was chosen. Accordingly, fuselage pitch and yaw, the main rotor controls θ_0, θ_C, θ_S and the tail rotor collective blade angle $\theta_{0, TR}$ form the set of six free variables besides the 88 generalized coordinates describing the elastic blade motion. HOST solves for these variables using a Newton-Raphson scheme to reach the trim objective consisting of an equal amount of conditions. The objective for free flight trim is to establish integral force and moment balance for the complete helicopter, i.e. to achieve a state of zero translational and rotational acceleration at a prescribed flight speed. As mentioned in the introduction, this trim objective differs from the "wind tunnel rotor trim" in that it demands varying rotor loads instead of prescribing fixed targets for a selection of the forces and moments generated at the rotor. By manipulation of the main rotor controls and of the helicopter pitch attitude, rotor thrust, propulsive force and roll/pitch moment are matched to the respective loads arising at the fuselage. With prescribed roll angle, balance of lateral force and yawing moment is mainly obtained by trading fuselage

sideslip angle and tail rotor thrust. Due to rotor-fuselage aerodynamic interference, and since the EC145 has a hingeless blade articulation that links the rotor's propulsive/lateral force and pitch/roll moment generation, a certain amount of coupling is introduced. HOST generally offers a wide variety of analytic models to describe interactions between various aerodynamic subcomponents. It is noted, however, that for the present case no representation of aerodynamic interaction between rotor and fuselage is activated, hence the influence of such effects on the flight state are contributed by CFD through load coupling (cf. reference [10]). Loads from skids, through skid-fuselage interference, and rotor hub loads, which are not covered by the CFD model, enter HOST as additional corrective terms. In the present case, lift and drag of the rotor hub and of the inner blade portions not represented in the CFD mesh are obtained from wind tunnel measurements. The values remain fix during trimming, no dependence on fuselage attitude is taken into account. Their impact on the first re-trim, i.e. when comparing trim 1 states with and without hub load correction, amounts to an increase of nose-down pitch attitude by 0.5°, to additional 0.2° of yaw to the left and to main rotor control angle changes by $\Delta\theta_0$=+0.37°, $\Delta\theta_C$=+0.15°, $\Delta\theta_S$=-0.27°.

Trim iterations are initiated by the first prediction of trim variables by HOST for the prescribed cruise flight condition at 136kts. The resulting set of attitude angles, rotor control angles and generalized coefficients describing blade motion is based solely on HOST internal aerodynamics and is termed trim 0. Subsequently, a FLOWer simulation of this trim state is carried out. At an early stage of this work only a preliminary version of the blade structural model was available in HOST, and as a consequence loads determined by FLOWer for trim 0 correspond to the preliminary trim state listed in Table 2. As the table shows, the update of the structural model brings about changes in the rotor controls of up to 0.84° and reduces the nose-down pitch attitude by 0.23°.

Table 2: Trim 0 with old and new blade structural model

Trim 0	θ_0-θ_{0FT}	θ_C-θ_{CFT}	θ_S-θ_{SFT}	$\theta_{0, TR}$	Θ	Ψ
Preliminary blade model	0.34°	-0.55°	2.65°	5.94°	-0.63°	-1.62°
New blade model	1.18°	-1.14°	3.02°	5.55°	-0.40°	-1.63°

Notwithstanding this profound change in the HOST model, results obtained with FLOWer on the preliminary trim 0 state may be used in the further course, provided the corrective term in eq. 2 is formed with the HOST loads F_{2D} obtained with the preliminary model. It is assumed that the aerodynamic correction is still approximately valid at the trim 0 state determined with the new structural model and serves sufficiently well to predict a useful trim update, which was confirmed by the subsequent trim progress. Trim iterations are continued by transferring the trim 1 state description to FLOWer, were the new rotor control angles and blade motion are instantly reset at the flow computation restart, whereas the fuselage gradually assumes its new attitude during the first quarter revolution. While the first reorientation occurs at a constant turning rate with abrupt turn initiation and termination, an improved motion law in the form $[d\Theta/dt; d\psi/dt] = 2\Omega \cdot \sin(2\Omega t) \cdot [\Delta\Theta; \Delta\psi]$ is used for all subsequent trim iterations. As soon as the flow reaches a certain level of convergence in its response to the new settings, aerodynamic loads are determined as the temporal mean over at least one main rotor period in case of fuselage loads, and as a phase average in case of the rotor. For all trim calculations of HOST following the initial trim 0, HOST loads are replaced by the CFD results F_{3D}^n. The internal aerodynamic model of the comprehensive helicopter code takes only the role of predicting load changes F_{2D}^{n+1}-F_{2D}^n at the blades and the fuselage, such that the trim Jacobian can be established. In case of a converged trim process, trim variable changes and load changes F_{2D}^{n+1}-F_{2D}^n tend to zero such that the corrective term F_{3D}^n-F_{2D}^n causes a complete replacement of the HOST internal aerodynamics by the FLOWer results. If a conservative load transfer can be assured, mean aerodynamic loads from CFD for the complete helicopter finally are in balance with helicopter weight.

In the present case five trim iterations were necessary to reach convergence within the accuracy limit of the scheme. Development of the trim variables is shown in Figure 6 and Figure 7, plotting main rotor control angles, tail rotor thrust and fuselage attitude. Convergence of blade motion can be recognized in Figure 8 from coincidence of blade tip path motion in trim 4 and 5. The total number of iterations required to reach convergence is well in the range known from "wind-tunnel trim" of isolated, torsionally stiff rotors, see for instance [2]. Initially a pronounced variation of trim variables takes place from trim cycle 0 to 1, which is caused by the substantial alteration of aerodynamic load modeling when adopting the correction terms from CFD. Any further changes from trim iteration n to n+1 are rooted in the differences between HOST prediction F_{2D}^n-F_{2D}^{n-1} and actual CFD response F_{3D}^n-F_{3D}^{n-1} and are smooth. A moderate overshoot in attitude and all rotor control angles except θ_S occurs, but no oscillations develop. With respect to blade motion, predominantly a change in longitudinal tip path plane tilt within the rotor mast system can be observed. A forward inclination of the plane compared to trim 0, which constitutes a compensation for load correction mainly at the fuselage, is followed by several increments of backward tilt that diminish as the final trim 5 is approached.
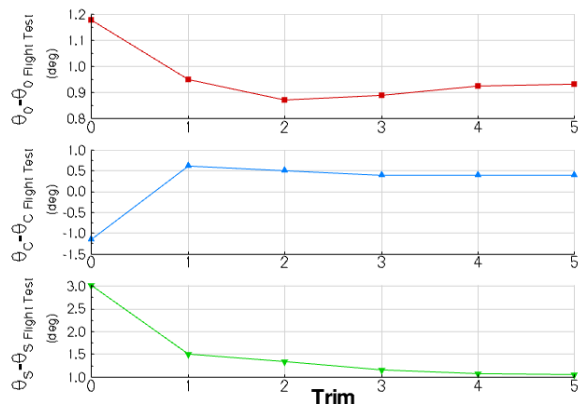
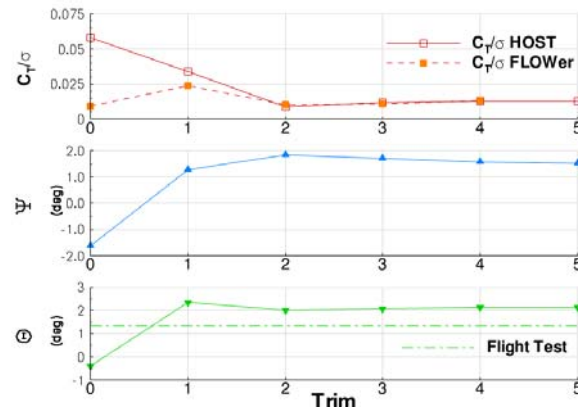**Figure 6: Trim convergence of main rotor control angles.**

Figure 7: Trim convergence of tail rotor thrust C_T/σ, fuselage yaw angle ψ and pitch attitude θ.
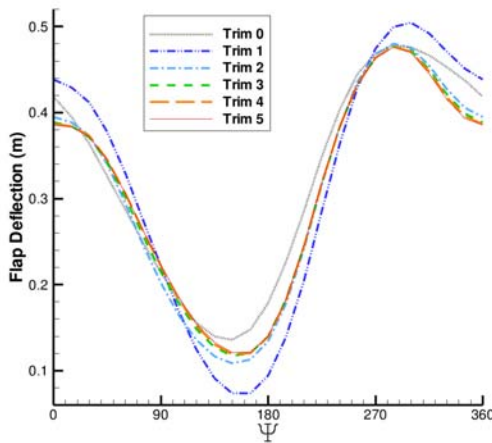

Figure 8: Trim convergence of tip flap deflection.

At the tail rotor, no load coupling between FLOWer and HOST is implemented to date, and therefore no control angle is transferred to FLOWer. Rather, tail rotor thrust in the CFD simulation was trimmed to the thrust level calculated by HOST based on a sensitivity study. The HOST value, ensuring yaw moment balance at the current trim iteration, is considered as objective for the manual setting of

tail rotor collective and is met at the last CFD simulation, in trim 4. Without load coupling, the main purpose of correct tail rotor thrust setting is to account for interference effects on the empennage. A CFD study of main rotor – tail rotor interference on tail rotor control can be found in [19]; imposing yaw moment balance, trimmed tail rotor collective settings at various forward and sideways flight conditions are monitored. Plotting the fluctuations of $\theta_{0,TR}$ with time and quantifying the unsteadiness of yaw moment generation, the study is also interesting in the context of trim accuracy.

Accuracy

Since a smooth development of the trim variables is observed, the convergence progress can be judged from variations at the final iteration. From trim 4 to trim 5, rotor controls vary by less than 0.02° and the fuselage attitude undergoes reorientations of less than 0.06° in yaw and 0.02° pitch. Representing blade motion, blade tip paths replace vertically by less than 0.003m. In comparison, for isolated rotor "wind tunnel trim" a convergence criterion of 0.01° change in rotor controls was applied in the past at our department. An impression of the proximity to the desired equilibrium flight state can also be gained from residual forces or accelerations. At trim 5, the remaining imbalance results in translational acceleration of less than 0.02m/s², and yaw, roll and pitch rate derivatives drop to -0.7deg/s², 0.3deg/s² and -0.8deg/s², respectively.

Convergence accuracy depends on the precision at which load changes due to trim variation are reproduced by the flow solver. In addition, if averaging is needed as in case of fuselage load coupling pursued in parallel to weak coupling of rotor loads, post-processing techniques eventually are relevant to analyze load signals that show lower or non-integer frequencies compared to the main rotor. With weak fluid-structure coupling being based on the exchange of periodic data, interaction of blade passing events with the natural shedding or oscillation frequencies of fuselage flow structures is likely to complicate averaging. The latter is particularly the case for main rotor – tail rotor interactions (cf. [19]), and for tail rotor – fuselage interference. Simple time averaging of fuselage loads and phase averaging of rotor loads reduces errors from non-matching frequencies if the mean is taken over a sufficiently extended interval, yet might be ineffective since it retards re-trimming and raises computational expenses. Nevertheless, averaging proved practicable in the present study and allowed for reasonable convergence accuracy, although at considerable computing effort. Besides more sophisticated signal analysis techniques, potential for accelerating the trim process might also be found in a careful choice of the appropriate instant for re-trimming. Early in the convergence process and particularly at the initial trim, the deviation of actual from trimmed state is large. Hence the aerodynamics and related correction terms forwarded to the aeromechanics code are approximate in general, unless the unlikely case of linear variation is encountered. Minimum requirement is that trim variable prediction reflects the general trend and

stability of the trim scheme is preserved. Increasingly higher accuracy is demanded when variations in trim variables diminish and the converged state is approached. Thus, through appropriate reduction of accuracy and flow convergence requirements at the initial cycles of the trim process, simulation time might be saved.

The impact of the corrective term and variations of it on the trim variables can be judged approximately from the trim Jacobian, which is given in eq. 3 based on the gradients of the HOST internal aerodynamic model for the trim 0 state. In this reduced form trim variables for blade motion are not listed.

$$
\begin{pmatrix}
0.45 & -2.34 & 0.28 & -0.03 & -0.10 & 0.06 \\
0.12 & -0.89 & -0.09 & 0.02 & 0.41 & -0.22 \\
-0.26 & 1.47 & -0.60 & 0.11 & 0.39 & 0.26 \\
0.28 & -3.75 & -2.89 & 1.80 & -0.62 & 0.06 \\
-0.02 & 0.97 & 3.40 & -0.52 & 0.60 & 0.00 \\
0.33 & 2.73 & 0.04 & -0.04 & -0.02 & -0.48
\end{pmatrix}
\begin{pmatrix}
\partial C_x \\
\partial C_y \\
\partial C_z \\
\partial C_{Mx} \\
\partial C_{My} \\
\partial C_{Mz}
\end{pmatrix}
=
\begin{pmatrix}
\partial \theta_0 \\
\partial \theta_c \\
\partial \theta_s \\
\partial \theta_{0,TR} \\
\partial \Psi \\
\partial \Theta
\end{pmatrix}
\qquad \textbf{eq. 3}
$$

Aerodynamic correction terms $F_{3D}{}^n$-$F_{2D}{}^n$ forwarded to HOST perturb the trim state defined by the trim objective of load equilibrium. HOST seeks to restore the equilibrium through compensation of the load perturbation and varies the state in order to generate an opposing vector $[\Delta C_x; \Delta C_y; \Delta C_z; \Delta C_{Mx}; \Delta C_{My}; \Delta C_{Mz}] = -(F_{3D}{}^n - F_{2D}{}^n)$. Note that from eq. 2 follows $-(F_{3D}{}^n - F_{2D}{}^n) = (F_{2D}{}^{n+1} - F_{HOST}{}^{n+1})$, with $F_{HOST}{}^{n+1}$ satisfying the trim objective. In analogy, deviations of the load correction term from its long term average $(F_{3D}{}^n - F_{2D}{}^n)_{temp} - (F_{3D}{}^n - F_{2D}{}^n)_{long\ term} \equiv -[\Delta C_x; \Delta C_y; \Delta C_z; \Delta C_{Mx}; \Delta C_{My}; \Delta C_{Mz}]$ provoke trim variable reactions of HOST that are approximately described by the locally valid Jacobian, provided the changes are sufficiently small. As the Jacobian indicates, perturbations in roll moment ΔC_{My} and in vertical force ΔC_x are in great parts compensated by suitable rotor control inputs. Note here that changes in the rotor control angles often induce a stronger response in the corresponding loads than equal changes of the attitude angles. In contrast, yawing moment ΔC_{Mx} and particularly lateral force perturbations ΔC_z induce principal response in yaw attitude and tail rotor collective. Similarly, longitudinal forces ΔC_y and pitching moment ΔC_{Mz} are linked to pitch attitude. Comparing these sensitivities to the fuselage forces determined by CFD allows an estimate on the variability to be expected for the attitude angles. In Figure 9 the development of total fuselage pitching moment is plotted for the entire trim process lasting 22 rotor revolutions, with re-trims indicated by vertical bars.
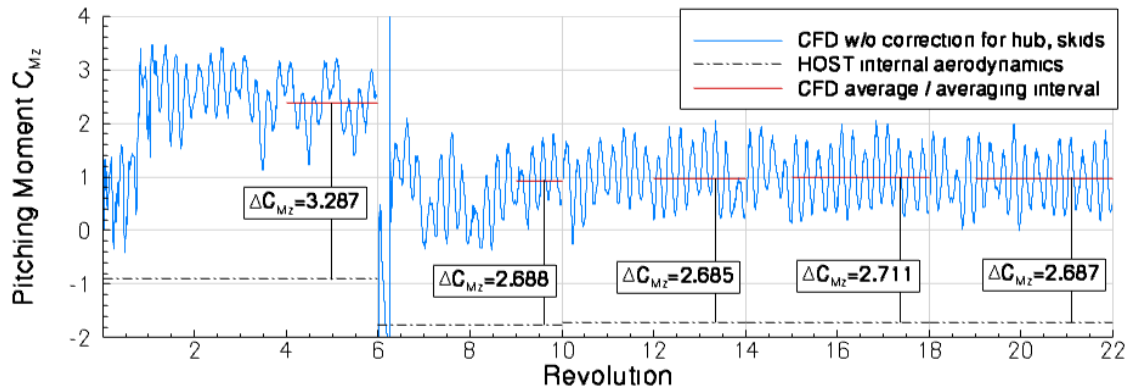

Figure 9: Fuselage pitching moment from CFD and HOST internal aerodynamics
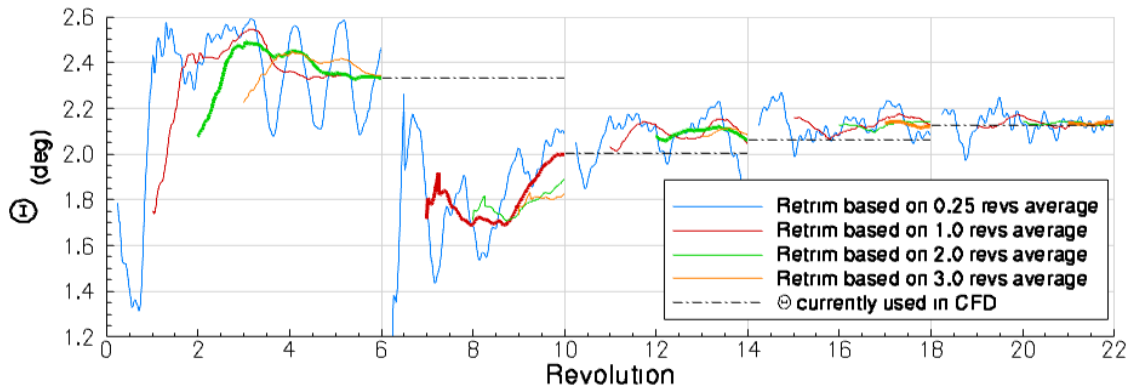

Figure 10: Continuous monitoring of trim variable Θ. Load averaging over different intervals.

Recall that each trim is initiated by reorienting the fuselage during one quarter of a revolution, resulting in high loads particularly at the beginning of trim 1, i.e. from rev. 6.00 until rev. 6.25. The signal is composed of 4/rev parts due to blade passing combined with fluctuations at frequencies subharmonic to 4/rev. Clear evidence for subharmonic content around 1/rev is found from rev. 3.00 onwards until the end of trim 0. Red lines mark the mean load coupled to HOST and obtained from averaging over an interval corresponding to the line length. The averaging interval for every fuselage load component is identical for a particular trim iteration and is chosen for each trim by inspecting the signals of all loads. In analogy, and unlike the common practice in "wind-tunnel trim", periodic rotor loads are obtained from phase averaging not only one but a corresponding amount of several periods. Averaging is started only after the flow presumably has converged to the new trim conditions, which is expected to last longer after starting the simulation from steady state and when reorienting the fuselage at high turn rates. Interval length is set according to the rising accuracy requirements when approaching convergence. Choice of an interval lasting 2.00 revolutions in trim 0 is due to the strong appearance of a subharmonic component. Dash-dotted lines below the CFD loads indicate the corresponding pitching moment determined HOST-internally. The boxed values are the mean offset between FLOWer and HOST, i.e. the aerodynamic correction term applied to the next trim. The considerable difference in pitching moment, with FLOWer generating nose-up moment in contrast to HOST, results in great part from higher negative lift on the horizontal stabilizer in the CFD simulation. No representation of the main rotor downwash effect was used on HOST side. Assuming that the tabulated aerodynamic data within HOST, which is obtained from wind tunnel experiments, approximates well the stabilizer lift gradient with Θ, the diminished correction term in trim 1 suggests that the magnitude of rotor-stabilizer interference changes with trim. From trim 1 onwards, where only small modifications in Θ take place (see Figure 7), the correction term remains nearly constant and thus fulfills the prerequisite for convergence of the scheme. The subharmonic pitching moment variations between rev. 3.00 and rev. 6.00 originate from lift changes at the horizontal stabilizer, see Figure 11, which however is not operating in stalled condition at any time.

Also at other fuselage components, for instance the cabin, rear door and tail boom, some traces of events at about 1/rev can be found. Main rotor lift as well contains a very small subharmonic component with an amplitude of ca. 0.025. With no fuselage turning applied at the beginning of the simulation, these subharmonics are probably launched by departing from a steady flow initial condition. At the stabilizer they decrease in later stages of the trim process (see Figure 11). Estimating the peak-to-peak amplitude of the subharmonic component in fuselage pitching moment to about 0.7 in trim 0, variations in fuselage pitch attitude of ca. $\Delta\Theta=0.35°$ can be expected from the trim Jacobian if this component is not filtered out.
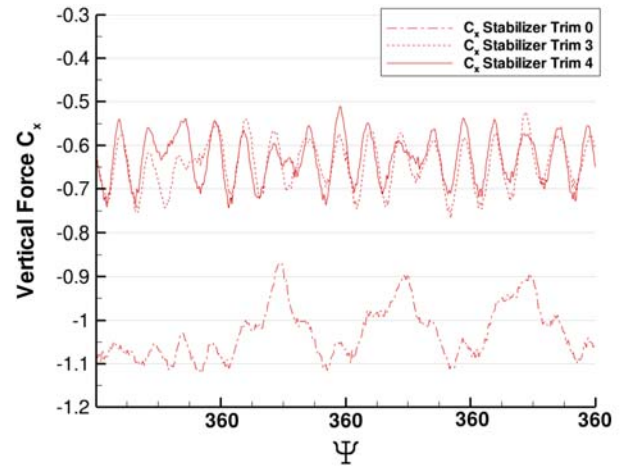

Figure 11: Lift on horizontal stabilizer in trim 3 and 4 and towards the end of trim 0.

A convenient method to assert the benefit from averaging or filtering techniques on convergence accuracy and rate is to continuously monitor the trim variables. To this end, a HOST trim calculation is carried out every 5 timesteps while the CFD simulation advances. Fuselage and rotor loads coupled to HOST are obtained from the immediate past, i.e. in the present study by averaging over a time interval reaching a certain number of periods backwards from the current timestep. The outcome, using intervals of ¼, 1, 2, and 3 main rotor revolutions, is shown one page earlier in Figure 10 for the Θ trim variable. For the present case continuous monitoring was applied only after all trim iterations were completed as an a-posteriori analysis. Hence the trim state used in CFD at the current iteration (dash-dot) is obtained as the last value from the preceding iteration, where the applied averaging is marked as a thick line. Several features of trim convergence are immediately observed; on one hand, pitching moment fluctuations and their mitigation by long-term averaging are clearly visible. On the other hand, convergence of the flow state towards the new trim can be checked. Furthermore, it is apparent that trim accuracy heavily depends on the averaging interval. If the mean was taken only over one quarter rotor period, as it is common practice at our department with isolated rotor trims, pitch attitude would be predicted with an accuracy of 0.5° in trim 1 and 0.2° at the final trim. As mentioned, a change in pitch of less than $\Delta\Theta=0.02°$ occurred from trim 4 to trim 5, which is the result of the high trim precision achieved through averaging over 3 rotor revolutions in trim 3 and 4. High-frequency oscillations at ca. 5/rev, observable particularly for 0.25 rev. averaging from rev. 10.00 onwards, might result from tail rotor influence.

Drag and lift forces were noted to have smaller subharmonic content and are less critical for trim accuracy. However, similar to pitching moment, also the fuselage lateral force and yawing moment contain fluctuations at

frequencies lower than 4/rev with considerable impact on yaw angle. Figure 13 shows fuselage lateral force C_z from FLOWer and HOST for the entire trim process, while Figure 14 plots the effects on yaw angle Ψ by continuous trim monitoring. Again, as for the pitching moment, subharmonics are clearly present from rev. 3.00 until rev. 6.00, and in trim 4 they seem to cause a modulation of the 4/rev part in the C_z signal. Corresponding yaw angle changes, which are also rooted in yaw moment oscillations, have a bandwidth of 0.5° for averaging a quarter rotor revolution in trim 0. Final trim precision achieved by averaging over 3.00 revolutions is ca. 0.03°, with an out-of-trim estimate of 0.06°.

Lateral forces at frequencies lower than 4/rev mainly originate from the tail boom and vertical control surfaces, as Figure 12 indicates for trim 0. Cabin loads, and remarkably also side forces on the rear door where flow separation occurs, are ¼ rev periodic. The offset between FLOWer and HOST loads is ΔCz=-0.575 at the initial trim. HOST predicts a lateral force to the right for the nose-left attitude since negative C_z at the cabin is outweighed by positive, rightward load on the canted endplates.
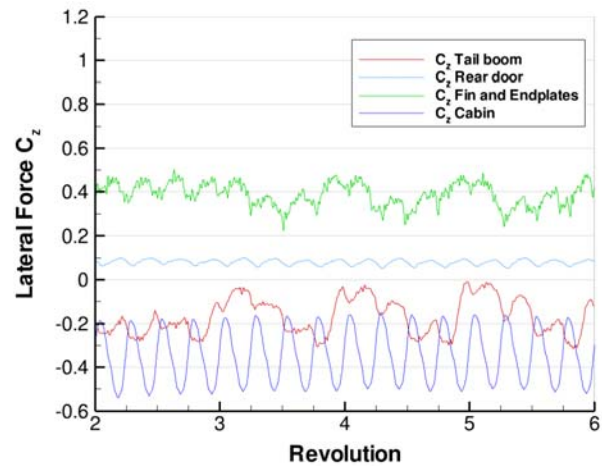

Figure 12: Lateral force on fuselage components, trim 0.

CFD yields significantly higher leftward cabin loads and also lower endplate lift, with the former causing the nose-right trim correction from trim 0 to trim 1. It is interesting to note that also in nose-right attitude the cabin produces leftward forces according to CFD.
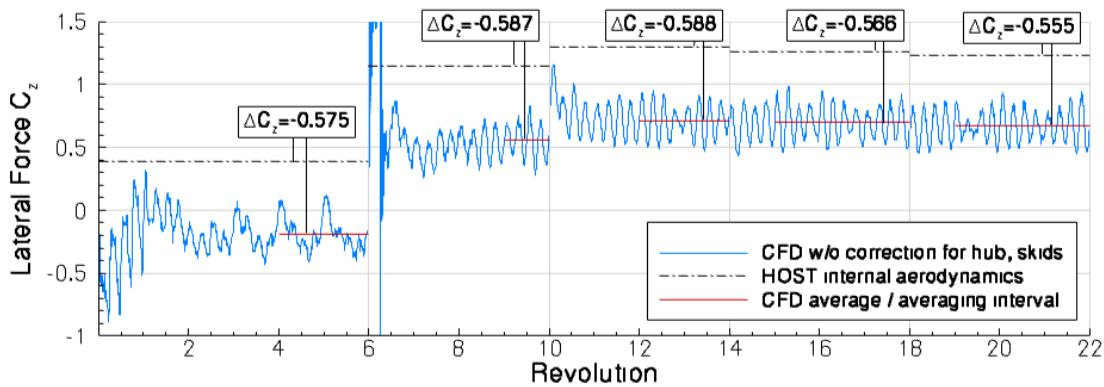

Figure 13: Fuselage lateral force from CFD and HOST internal aerodynamics
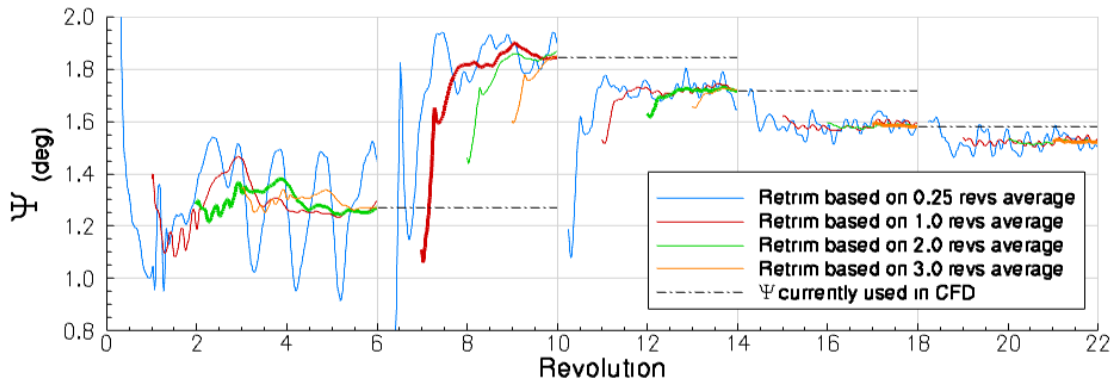

Figure 14: Continuous monitoring of trim variable Ψ. Load averaging over different intervals.

Computational effort

Not counting the simulation time spent for determining the skid load and interference effects, 22 rotor revolutions were required to conduct free flight trimming. CFD simulations were mainly carried out on a NEC SX-8 vector computer and later on a NEC Nehalem cluster, both installed at the high performance computing center HLRS in Stuttgart. Calculations on the NEC SX-8 were set up for parallel use of 16 processors or 2 nodes, and ca. 23.2 h of wallclock time were spent on one rotor revolution. On the Nehalem cluster good performance was achieved with 60 parallel processes, although the limit for equal load balancing between all blocks of the mesh system, which was designed for the vector computer, is reached already at 32 processes. Due to memory requirements, only 4 out of 8 cores per node were in use. Simulation of one rotor revolution requires ca. 18h of wallclock time, with a share of Chimera connectivity calculations of less than 10%. Accordingly, total computational effort for the entire trim would amount to ca. 8.200 CPU-hours in case that solely the vector computer was used, compared to ca. 24.000 CPU-hours on the cluster.

Computation time might be saved by carefully setting relaxed accuracy requirements at the early phase of the trim process, and by selecting an appropriate instant for re-trimming, as stated earlier. Inspecting once more the development of the trim variables Ψ and Θ shown by continuous monitoring in Figure 10 and Figure 14, it seems possible to reduce FLOWer trim 0 simulation duration from six to only four revolutions. If averaging over one revolution is applied, nearly the same values for Ψ and Θ are obtained. This is also observed for other trim variables such as the rotor controls. With respect to the great departure from the HOST initial trim 0, which provided the starting values $\Psi=-1.63°$ and $\Theta=-0.40°$ (see also Figure 7), it even might be advisable to further shorten the FLOWer simulation for the trim 0 state to about two revolutions, and to spend the time saved on an intermediate state closer to trim 1. At this intermediate state, a better estimate for the actually required aerodynamic correction is obtained, while it is not effective to calculate aerodynamic correction terms at high precision for a state far from convergence. Generally, trim precision and also flow convergence are less important the more the subsequent trim departs from the current state. For revolutions 6.00 to 10.00, different conclusions on the appropriate instant of re-trimming can be drawn from the Ψ and Θ development; while the yaw angle settles early and allows re-trim approximately at revolution 8.00, the pitch angle still develops. Since it re-approaches the currently used value, it seems worthwhile not to interrupt the simulation prematurely. Trim 3 and 4 values are well estimated from simulating only three revolutions using the last two ones to form mean loads. At the last trim, the high accuracy gained from averaging over three revolutions is needed. Retrospective, about four to five revolutions could likely have been saved from the total simulation time.

Stability

In light of the significant deviations of CFD determined fuselage loads from the HOST model, an exemplary, approximate stability analysis for the convergence of the lateral balance of forces, and for the yawing moment, shall be given here. For the present work, the coupling and trim scheme is based on delta trimming in its basic form without any relaxation. The change in trim variables is predicted by the Newton-Raphson scheme through repeated use of trim Jacobians that are established from the comprehensive rotor code's internal models. The contribution from CFD is to indicate the current out-of-trim state $F_{3D}^n–F_{HOST}^n$. In the derivation of the trim Jacobian, only the gradient of the aerodynamic load over trim variable change is relevant, as much as no absolute aerodynamic load but only the difference $F_{2D}^{n+1}-F_{2D}^n$ determines the change in trim predicted by HOST after some Newton-Raphson iterations. It is apparent that the accuracy of the prediction depends on the fidelity of the lower order (surrogate) aerodynamic model in HOST to the CFD model in terms of the gradient over trim variable change. Convergence to the objective is ensured, if the CFD gradient in the direction of trim change is of equal sign, and if it compares in magnitude by a ratio of less than two. If the former condition is not satisfied the trim diverges. If the CFD load response to trim variable change exceeds the respective lower order model sensitivity during several trim iterations, oscillations develop, which are decaying only for a FLOWer to HOST sensitivity ratio of less than two.

In Figure 15 the HOST value for lateral aerodynamic force C_z at the fuselage is plotted over yaw angle Ψ, and compared to CFD values available for the five computed trim states. Gradients with Ψ compare well and show little dependence from fuselage pitch angle Θ. To estimate the stability boundary for the CFD fuselage load gradient at trim 0, the local trim Jacobian was determined. As outlined before, HOST seeks to restore the load equilibrium by trim variations that cause load changes $[\Delta C_x; \Delta C_y; \Delta C_z; \Delta C_{Mx}; \Delta C_{My}; \Delta C_{Mz}]$ opposing the perturbation induced by the aerodynamic correction term $F_{3D}^n-F_{2D}^n$. Taken the simplified case that the only inconsistency between CFD and the low-fidelity model consisted in a different prediction of the lateral force, a trim perturbation only in C_z would occur; convergence would depend on the degree to which the required compensation ΔC_z is realized in CFD with the proposed trim variable change. Requirements are equal sign and less than twofold magnitude, i.e. $\Delta C_{z,\ FLOWer} = [0…2\Delta C_{z,\ HOST}]$. With C_z being the global aerodynamic load on the helicopter, ΔC_z is composed of lateral force changes at the fuselage, the main rotor and the tail rotor. Further assuming generously that main and tail rotor forces are truly modeled in HOST, the entire stability margin becomes available for fuselage load prediction. This results in the stability boundaries included in Figure 15, with a negative lift gradient allowed at the divergence limit since $\partial C_z/\partial \Psi$ at the rotors are positive.
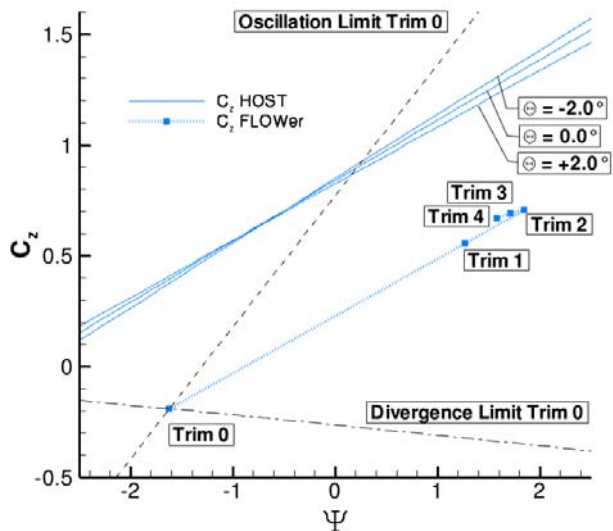
Figure 15: Fuselage lateral force variation with trim state for HOST and FLOWer, stability margin.

Figure 16: Fuselage yaw moment variation with trim state for HOST and FLOWer, stability margin.

With degraded modeling accuracy at the latter components, the stability margin for fuselage load prediction narrows. Note that the abscissa in Figure 15 represents a trim change which consists also in variation of trim variables besides Ψ and Θ, cf. the Jacobian eq. 3. For the analysis presented, it was assumed that the discrepancy between CFD and the empirical-based model is suitably described by relating load differences to the neutral point of fuselage lateral aerodynamics in HOST. Hence, the corresponding Jacobian is used, and trim perturbation ΔC_z due to fuselage modeling difference can be imagined to attack at the neutral point, which lies somewhat behind the main rotor axis. Also note that the stability analysis is limited in that it is only exact in the validity area of the Jacobian.

In analogy a stability analysis for the fuselage yaw moment about the neutral point is carried out. Figure 16 shows notably different gradients of fuselage C_{Mx} with yaw attitude, which indicates that the neutral point of the CFD model is located further rearwards. Stability against trim divergence is ensured, as long as yaw moment generation foreseen by HOST remains effective also in CFD. Since in the present case with prescribed roll attitude yaw moment generation about the neutral point works predominantly by tail rotor thrust, this is the case as long as the neutral point of the CFD model stays in front of the tail rotor, a requirement that is fulfilled easily. Equally ample stability is provided against oscillations in the trim scheme, which only would occur if the CFD neutral point settled approximately twice as far from the tail rotor as in the HOST model.

Note, that again consistent modeling of the components besides the fuselage was assumed. If tail rotor loads from CFD were coupled, differing thrust gradients would narrow the stable region.
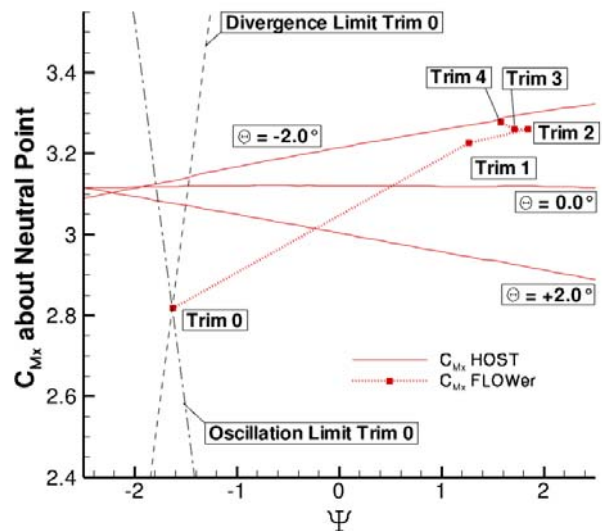
COMPARISON TO FLIGHT TEST DATA

In Figure 6, trim variable convergence is plotted as offset from the control settings measured in the flight test, while in Figure 7 the pitch attitude reference is included as dashed line. Recall that the yaw angle was not registered in flight testing. For all main rotor control angles and also for the fuselage pitch attitude, a better reproduction of the flight test values is achieved after replacement of comprehensive code aerodynamics by the CFD results, as can be seen by comparing final and initial trim states. This remains true also if the additionally coupled hub loads are provided to HOST for the initial trim; as stated earlier, hub drag and lift change the helicopter attitude by approximately 0.5° additional nose-down pitch, accompanied by an increase in main rotor collective θ_0 by 0.37°. Both changes mean a further departure of the trim 0 state from the measured data. However, HOST stand-alone prediction of main rotor cyclic control angle benefits from hub load consideration. In HOST, induced velocities in the rotor plane were calculated with a Meijer-Drees model.

Comparison of the trimmed CFD results to flight test data is a difficult task, since it effectively means a verification not only of flow solving accuracy, but also of load conservation in coupling and exactness in blade structural and dynamic modeling. Tracing back any discrepancies is very difficult due to the strong interrelation of all phenomena while the only fixed conditions are flight speed and load equilibrium. Therefore, an in-depth analysis has not been attempted so far but is planned for the future. Nevertheless, some sources of discrepancies shall be listed. first of all, no mass flux through the engines was considered. The closed engine inlet and missing exhaust momentum certainly increase drag, and no interference of the exhaust plume with the empennage and the rotor takes place. See also [20] and [21] for a discussion of engine

effects. Furthermore, guerney flaps at the horizontal stabilizer and small strakes along the tail boom are not present in the geometrical model. Last but not least it is recalled that skid loads and in particular the related interference effect are estimated from the trim 0 flight condition, with the considerable lateral force, rolling and yawing moment precluded from the load coupling.

CONCLUDING REMARKS

With the present study, free flight trim of a complete helicopter CFD model including aeroelastic blade deformation was shown feasible. For the chosen cruise flight case, moderate interference effects between rotor and fuselage are encountered, which justify the expensive use of CFD for flight attitude prediction, particularly for parts where interference changes with trim, as was shown for the horizontal stabilizer. Furthermore, separate modeling of the components in an empirical-based aerodynamics approach is also questioned when considering results from a simulation including the skids, where interference effects were shown to partly exceed the primary influence. With regard to the flight test data available for the studied condition, a significant improvement from replacing the low-fidelity aerodynamic model in the comprehensive rotor code by CFD is registered for all control angles and the fuselage attitude.

Convergence rate of the expanded trim scheme is comparable to "wind tunnel trimming" of an isolated rotor in terms of trim iterations for the investigated flight condition. Computational effort, however, is considerable, but there is some indication that a reduction in effort might be achieved through timely advancement of the trim state in early phases of the trim process by carefully relaxing the requirements on flow convergence and accuracy. A continuous monitoring of trim variable development during runtime of the CFD simulation is suggested that provides help in identifying the appropriate instant for stepping forward to a new trim cycle.

The CFD simulation of the EC145 helicopter with its specific bluff fuselage was characterized by considerable fluctuations in fuselage pitching moment and lateral force with non-negligible impact on trim. Less on the rear door itself, yet particularly on the tail boom and empennage, dynamic loads were noticed at frequencies subharmonic to blade passage. To ensure adequate trim precision, the averaging interval of one rotor period typically used in weak coupling is extended over several periods for both fuselage and main rotor loads. This also helps to reduce the error due to non-integer frequency ratios of fuselage and tail rotor load components with respect to main rotor load. The benefit from various averaging techniques can be observed with the continuous monitoring of trim variable prediction during the CFD simulation. More sophisticated signal analysis techniques may help to reduce the averaging period required and thus improve computational effort.

With regard to stability of the weak coupling and trim scheme, a smooth development of control angles and two examples of a simplified stability analysis indicate that, despite considerable correction of the HOST aerodynamics through the fuselage load coupling, a stable convergence of the trim process can be expected for the complete helicopter trim. Difficulties however may appear when rotor-fuselage interference effects considerably modify fuselage load gradients. The low-speed pitch-up condition for instance, with the stabilizer load heavily depending on its position in rotor downwash, might lead to a divergent trim. Also the tail-shake phenomenon that eventually might appear when including rotor hub models into CFD might require special treatment. In this context it generally seems advisable to include all devices that were foreseen at the real helicopter to cure flight mechanic instability or vibration problems.

ACKNOWLEDGMENTS

REFERENCES

1. Datta, A., Nixon, M. and Chopra, I., "Review of Rotor Loads Prediction with the Emergence of Rotorcraft CFD", Extended version of the paper presented at the 31st European Rotorcraft Forum, Florence, Italy, September 12-15, 2005, Journal of the American Helicopter Society, October 2007, Vol. 52, No. 4, pp. 287-317.

2. Dietz, M., Krämer, E., Wagner, S. and Altmikus, A., "Active Rotor Performance Investigations Using CFD/CSD Weak Coupling", Proceedings of the 34th European Rotorcraft Forum, Kazan, Russia, September 11-13, 2008.

3. Sheridan, P. and Smith, R., "Interactional Aerodynamics – A New Challenge to Helicopter Technology", Presented at the 35th Annual National Forum of the American Helicopter Society, May, 1979.

4. Costes, M., Raddatz, J., Borie, S., D'Alascio, A., Embacher, M.: "Advanced Rotorcraft Aeromechanics Studies in the French-German SHANEL Project", Proceedings of the 35th European Rotorcraft Forum, Hamburg, Germany, September 2009.

5. Dietz, M., Maucher, C. and Schimke, D.,"Adressing Today's Aeromechanic Questions by Industrial Answers", Presented at the American Helicopter Society Aeromechanics Specialists' Conference, San Francisco, CA, January 20-22, 2010.

6. Datta, A., Sitaraman, J., Chopra, I. and Baeder, J.D., "CFD/CSD Prediction of Rotor Vibratory Loads in High-Speed Flight", Journal of Aircraft, Vol. 43, No. 6, November-December 2006, pp. 1698-1709.

7. Datta, A. and Chopra, I., "Prediction of the UH-60A Main Rotor Structural Loads Using Computational Fluid Dynamics/Comprehensive Analysis Coupling", presented at the 32nd European Rotorcraft Forum, Maastricht, The Netherlands, September 12-14, 2006.

8. Rajmohan, N., Manivannan, V., Sankar, L., Costello, M. and Bauchau, O., "Development of a Methodology for Coupling Rotorcraft Aeromechanics and Vehicle Dynamics to study Helicopters in Maneuvering Flight", presented at the American Helicopter Society 65th Annual Forum, Grapevine, Texas, May 27-29, 2009.

9. Bhagwat, M., Dimanling, A., Saberi, H., Meadowcroft, E., Panda, B. and Strawn, R., "CFD/CSD Coupled Trim Solution for the Dual-Rotor CH-47 Helicopter Including Fuselage Modeling", Presented at the American Helicopter Society Specialist's Conference on Aeromechanics, San Francisco, CA, January 23-25, 2008.

10. Borie, S., Mosca, J., Sudre, L., Benoit, C. and Péron, S., "Influence of rotor wakes on helicopter aerodynamic behaviour", Proceedings of the 35th European Rotorcraft Forum, Hamburg, Germany, September 22-25, 2009.

11. Kroll, N., Rossow, C.-C., Becker, K., Thiele, F.: "The MEGAFLOW Project", Aerospace Science and Technology, No. 4, 2000, pp. 223-237.

12. Costes, M., Pahlke, K., D'Alascio, A., Castellin, C., Altmikus, A.: "Overview of results obtained during the 6-year French-German CHANCE project", AHS 61st Annual Forum, Grapevine, TX, June 2005.

13. Jameson, A., Schmidt, W. and Turkel, E.: "Numerical Solutions of the Euler Equations by Finite Volume Methods Using Runge-Kutta Time-Stepping Schemes", AIAA-Paper 81-1259, 1981.

14. Jameson, A.: "Time Dependent Calculation Using Multigrid, With Applications to Unsteady Flows Past Airfoils and Wings", AIAA-Paper 91-1596, 1991.

15. Schwarz, Th.: "The Overlapping Grid Technique for the Time-Accurate Simulation of Rotorcraft Flows", Proceedings of the 31st European Rotorcraft Forum, Florence, Italy, September 2005.

16. Dietz, M.: „Simulation der Umströmung von Hubschrauberkonfigurationen unter Berücksichtigung von Strömungs-Struktur-Kopplung und Trimmung", PhD Thesis, Verlag Dr. Hut, ISBN 978-3-89963-942-1, 2009.

17. Benoit, B., Dequin, A-M., Kampa, K., Grünhagen, W. v., Basset, P-M., Gimonet, B.: "HOST: A General Helicopter Simulation Tool for Germany and France", American Helicopter Society, 56th Annual Forum, Virginia Beach, Virginia, May 2000.

18. D'Alascio, A., Castellin, C. and Schöning, B., "Industrial Validation of CFD Solvers on Medium and Large Helicopter Fuselages", Proceedings of the 31st European Rotorcraft Forum, Florence, Italy, September 13-15, 2005.

19. Fletcher, T. M. and Brown, R. E., "Main Rotor-Tail Rotor Interaction and Its Implications for Helicopter Directional Control", Journal of the American Helicopter Society, April 2008, Vol. 53, No. 2, pp. 125-138.

20. O'Brien, D. M. Jr., Calvert, M. E. and Butler, S. L., "An Examination of Engine Effects on Helicopter Aeromechanics", presented at the American Helicopter Society Specialists' Conference on Aeromechanics, San Francisco, CA, January 23-25, 2008.

21. Le Chuiton, F., "Quasi-Steady Simulation of a Complete EC-145 Helicopter: Fuselage + Main/Tail Actuator Disks + Enginges", 31st European Rotorcraft Forum, Florence, Italy, September 12-15, 2005.